Electrical Power and Energy Systems 35 (2012) 74–82

Contents lists available at SciVerse ScienceDirect

Electrical Power and Energy Systems

journal homepage: www.elsevier.com/locate/ijepes

Security-constrained transmission switching with voltage constraints

Amin Khodaei, Mohammad Shahidehpour *

ECE Department, Illinois Institute of Technology, United States

ARTICLE INFO

Article history:
Received 21 March 2011
Received in revised form 23 August 2011
Accepted 5 September 2011
Available online 17 November 2011

Keywords:
Transmission switching
Security-constrained unit commitment
Voltage constraints
FACTS devices

ABSTRACT

Transmission switching (TS) would play a vital role in the security and economics of electric power systems. The application of TS to the AC model of security-constrained unit commitment (SCUC) for the day-ahead scheduling is presented in this paper. The proposed AC model of SCUC with TS would include real and reactive power flow constraints which increase the controllability of base case and contingency solutions with voltage constraints. A general FACTS model is introduced for the reactive power management in SCUC which is based on the power injection model (PIM). A modified Newton–Raphson power flow model is introduced in the proposed SCUC with TS in which line flows are considered as variables. The proposed AC network model is compared with the DC network model for enhancing the power network controllability and minimizing the operation cost. The case studies exhibit the effectiveness of the TS application to SCUC with AC network constraints.

1. Introduction

Recent market design proposals consider a more active role for transmission owners. Incentives are provided for transmission owners to increase investments in transmission and to utilize transmission lines more efficiently. Considering that building new transmission lines to meet the growing demand is a difficult and time-consuming task, the more efficient use of the existing transmission network would be a valuable alternative. Transmission switching (TS) is an efficient approach to utilize the power grid more comprehensively. TS will take specific transmission lines temporarily out of service in order to benefit from the modified network topology. This capability will be considered primarily for the newly installed transmission lines in the electricity market. TS has gained further attention since the FERC order 890 has called for an economic utilization of transmission capacity and hence made TS more favorable for economic purposes. The independent system operator (ISO) may apply TS as a corrective action for mitigating transmission flow violations [1–4], as a congestion management tool [5], for enhancing the power system security [6–9], and improving the system economics while maintain the security constraints [10]. TS would manage topology changes which could affect nodal prices, load payments, generation revenues, congestion costs, and flowgate prices. It can also improve the solution of the capacity expansion planning problem while providing economic benefits [11,12].

Much of the previous studies considered the TS for real power flow adjustments. In this paper, the optimal TS is considered for mitigating both transmission flow and bus voltage violations in the security-constrained unit commitment (SCUC) problem. To consider voltage constraints, a modified Newton–Raphson model is utilized which will satisfy the base case and contingency constraints. The proposed SCUC solution uses the Benders decomposition to decompose the model into a master problem and two subproblems [13–17]. A general model of FACTS devices is incorporated in the proposed SCUC formulations, which is capable of modeling all types of series, shunt or shunt-series FACTS devices. These features will add a comprehensive perspective to the SCUC formulation for TS applications.

Fig. 1 depicts the flowchart of the proposed SCUC model with AC network constraints. Benders decomposition is utilized to decompose the SCUC problem into smaller and easier to solve subproblems. The master problem uses the available market information to find the optimal hourly schedule of units (UC) by considering the prevailing UC constraints [18–20]. The hourly solution of UC is used in the subproblems to examine the AC network constraints. The TS ability of lines is considered and FACTS devices are incorporated in the subproblems if violations are detected. TS binary variables are determined via UC and consequently, they are considered as constant values in the subproblems. Given the unit and line schedule by the UC solution, the Subproblem 1 will check the base case network feasibility. In this subproblem, slack variables for real and reactive power mismatches are minimized based on line flow and FACTS device adjustments. The proposed Benders cut incorporates slack variables for the real and reactive power mismatch that is mitigated by recalculating the unit and line schedules. A converged base case power flow will be achieved based on the UC results. The Contingencies Network Check subproblem, i.e., Subproblem 2, uses the UC solution for the base case

* Corresponding author.
E-mail address: ms@iit.edu (M. Shahidehpour).

0142-0615/$ - see front matter © 2011 Elsevier Ltd. All rights reserved.
doi:10.1016/j.ijepes.2011.09.014

Nomenclature

Indices

b, m, n	indices for bus
c	index for contingency
i	index for generator
l	index for line
ns	index for non-switchable line
s	index for switchable line
Sh	superscript for shunt power injections
Se	superscript for series power injections
t	index for time

Sets

B_b	set of FACTS devices connected to bus b
L_b	set of lines connected to bus b
U_b	set of units connected to bus b

Parameters

M	large positive constant
NB	number of buses
NG	number of units
NNS	number of non-switchable lines
NS	number of switchable lines
NT	number of time periods
PL_l^{max}	real power flow limit of line l
Q_i^{min}, Q_i^{max}	reactive power generation limits of unit i
UX_{it}	contingency state of unit i at time t
UY_{lt}	contingency state of line l at time t
V_b^{min}, V_b^{max}	voltage magnitude limits of bus b
α_b	power injection coefficient of FACTS device
δ_i^{max}	standing phase angle difference limit of line l
Λ_i	permissible real power adjustment of unit i

Variables

I_{it}	commitment state of unit i at time t
$MP_{bt,1}$, $MP_{bt,2}$	slack variables for real power mismatch in bus b at time t
$MQ_{bt,1}$, $MQ_{bt,2}$	slack variables for reactive power mismatch in bus b at time
P_{it}	real power generation of unit i at time t
PF_{bt}	real power injection in bus b at time t due to FACTS device
PL_{lt}	real power flow of line l at time t
Q_{it}	reactive power generation of unit i at time t
QF_{bt}	reactive power injection in bus b at time t due to FACTS device
QL_{lt}	reactive power flow of line l at time t
V_{bt}	voltage magnitude of bus b at time t
w_t	total mismatch at time t
z_{lt}	switching state of line l at time t
θ_{bt}	voltage angle of bus b at time t
ψ_{it}, μ_{lt}, π_{it}	dual variables

Symbols

$\wedge$	given variables

Matrices and vectors

$\mathbf{1}$	vector of ones
$\mathbf{A}$, $\mathbf{B}$, $\mathbf{C}$, $\mathbf{D}$	Jacobian matrices
$\mathbf{dP_0}$	real power mismatch vector
$\mathbf{dQ_0}$	reactive power mismatch vector
$\mathbf{MP_1}$, $\mathbf{MP_2}$	vector of slack variables for real power mismatch
$\mathbf{MQ_1}$, $\mathbf{MQ_2}$	vector of slack variables for reactive power mismatch
$\mathbf{X}$	bus-line incidence matrix
$\mathbf{Y}$	bus-unit incidence matrix
$\mathbf{\Delta P}$	real power generation increment vector
$\mathbf{\Delta PL}$	real power flow increment vector
$\mathbf{\Delta PL^{min}}$, $\mathbf{\Delta PL^{max}}$	real power flow lower and upper increment vectors
$\mathbf{\Delta Q}$	reactive power generation increment vector
$\mathbf{\Delta Q^{min}}$, $\mathbf{\Delta Q^{max}}$	reactive power generation lower and upper increment vectors
$\mathbf{\Delta QL}$	reactive power flow increment vector
$\mathbf{\Delta V}$	bus voltage increment vector
$\mathbf{\Delta V^{min}}$, $\mathbf{\Delta V^{max}}$	bus voltage lower and upper increment vectors
$\mathbf{\Delta\theta}$	bus phase angle increment vector
$\mathbf{\Delta\Lambda^{min}}$, $\mathbf{\Delta\Lambda^{max}}$	real power generation adjustment lower and upper increment vectors

to check the system security in case of contingencies. Using AC power flow equations, both real and reactive power mismatches are minimized in this subproblem. It is required to limit the standing phase angle difference to safeguard the rotor shaft. Different approaches are proposed to obtain the minimum generation redispatch in a reasonable time for desired standing phase angles [21–26]. This problem which is inevitable in restoration practices may also occur in the normal operation of power systems when attempting to reclose a single line that is a part of a transmission loop [23]. To present a practical TS model, the standing phase angle difference limit of switchable lines is formulated in our proposed model.

FACTS devices are incorporated here in the SCUC model. FACTS devices are traditionally modeled by a voltage (current) source model (VSM). VSM formulates the device according to the operating conditions, thus representing the device intuitively. However, it destroys the symmetric characteristics of the admittance matrix and may cause oscillations in the power flow solution in successive iterations. A more common approach, as used in this paper, is to utilize power injection model (PIM). The PIM is derived from VSM, in which real and reactive power injections are considered as independent control variables, as shown in Fig. 2. Using PIM, the symmetric characteristics of admittance matrix is kept and the oscillations in the power flow solution are mitigated. Due to advantages of the PIM, this model were extended to almost all FACTS devices and used in most of the researches on operation and control of power systems with FACTS devices. Table 1 represents the required PIM components for modeling different FACTS devices. The power injections are only interim results, where they would be converted to the corresponding VSM parameters once the solution is obtained. The control parameters and the required conversion to obtain control parameters from PIM components are not listed in the table since it can be found in the literature.

The rest of the paper is organized as follows. Section 2 presents the formulation of the problem. Section 3 conducts the numerical simulations and in detail discusses results obtained for the IEEE 118-bus system. Finally, concluding remarks are drawn in Section 4.

2. Security-constrained reactive power formulation

The step by step procedure for the solution of the proposed SCUC model is given as follows.

2.1. UC (optimal hourly schedule of units)

The UC solution provides the hourly generation dispatch and the state of switchable lines in both base case and contingencies.

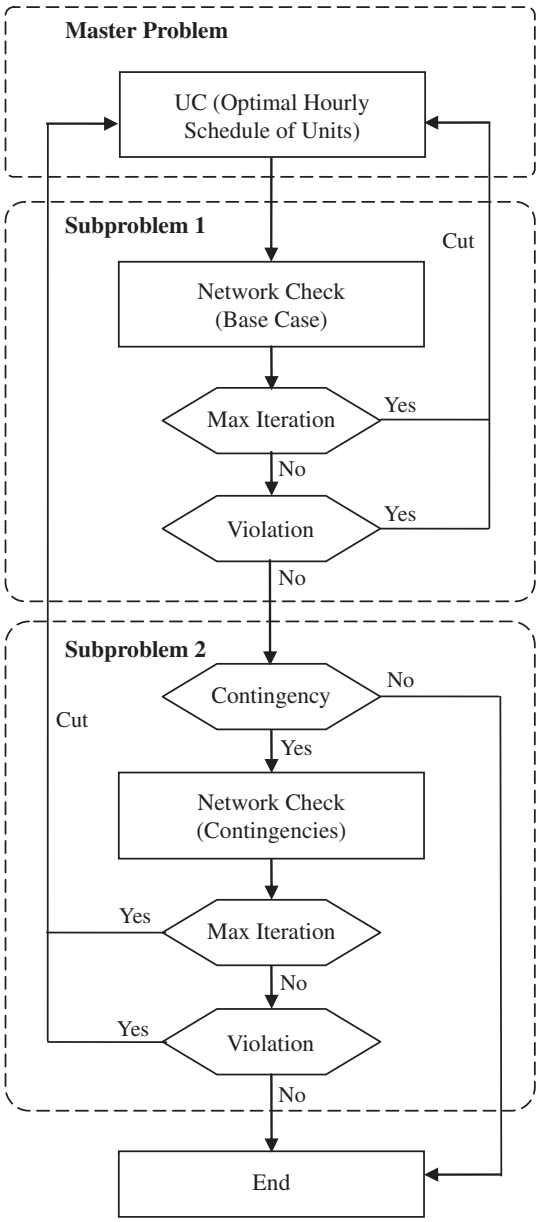

Fig. 1. Flowchart of SCUC with TS for reactive power management.

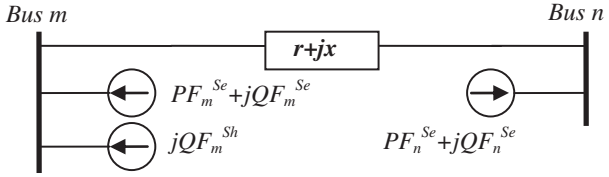

Fig. 2. Power injection model of FACTS devices.

At the first iteration of the problem, there is no constraint on switchable lines states. So, random initial values might be assigned to these variables. However, in our approach we consider that all lines are in service at the first iteration. In subsequent iterations, the Benders cuts from the subproblems establish more constraints on switchable lines states. Although the switchable lines states are determined in the master problem, they are actually governed by Benders cuts stemmed out of the subproblems. Mixed-integer programming (MIP) is used to formulate the UC problem.

2.2. Network check (general formulation)

In the Base Case and Contingencies Network Check subproblems, a linearized AC power flow based on Newton–Raphson method is performed to check the existence of a converged solution. The general formulation of this linearized power flow in matrix form is expressed by (1)–(8).

$$\mathbf{Min\,w}(\widehat{\mathbf{I}},\widehat{\mathbf{P}}) = \mathbf{1}^{\mathbf{T}}(\mathbf{MP_1}+\mathbf{MP_2}) + \mathbf{1}^{\mathbf{T}}(\mathbf{MQ_1}+\mathbf{MQ_2}) \tag{1}$$

$$\begin{bmatrix}\mathbf{Y}*\mathbf{\Delta P}\\ \mathbf{Y}*\mathbf{\Delta Q}\end{bmatrix} - \begin{bmatrix}\mathbf{X}*\mathbf{\Delta PL}\\ \mathbf{X}*\mathbf{\Delta QL}\end{bmatrix} + \begin{bmatrix}\mathbf{MP_1}\\ \mathbf{MQ_1}\end{bmatrix} - \begin{bmatrix}\mathbf{MP_2}\\ \mathbf{MQ_2}\end{bmatrix} = \begin{bmatrix}\mathbf{dP_0}\\ \mathbf{dQ_0}\end{bmatrix} \tag{2}$$

$$\begin{bmatrix}\mathbf{\Delta PL}\\ \mathbf{\Delta QL}\end{bmatrix} = \begin{bmatrix}\mathbf{A} & \mathbf{B}\\ \mathbf{C} & \mathbf{D}\end{bmatrix}\begin{bmatrix}\mathbf{\Delta\theta}\\ \mathbf{\Delta V}\end{bmatrix} \tag{3}$$

$$\mathbf{\Delta Q}^{\min} \leqslant \mathbf{\Delta Q} \leqslant \mathbf{\Delta Q}^{\max} \tag{4}$$

$$\mathbf{\Delta PL}^{\min} \leqslant \mathbf{\Delta PL} \leqslant \mathbf{\Delta PL}^{\max} \tag{5}$$

$$\mathbf{\Delta V}^{\min} \leqslant \mathbf{\Delta V} \leqslant \mathbf{\Delta V}^{\max} \tag{6}$$

$$\mathbf{\Delta P} = \mathbf{0} \tag{7}$$

$$\mathbf{\Delta\Lambda}^{\min} \leqslant \mathbf{\Delta P} \leqslant \mathbf{\Delta\Lambda}^{\max} \tag{8}$$

The AC power flow will converge when real and reactive power mismatches at each bus are zero. The objective function (1) minimizes the slack variables for real and reactive power mismatches in the system (2). In this formulation, instead of using the common form of Jacobian matrix [27], the line real and reactive power flows are incorporated in the power balance equation. The line flows are linked to power injections/withdrawals at the associated buses. The line flows are calculated based on bus voltage magnitudes and angles as presented by (3). This modification does not change the basic power flow formulation while it enables the modeling of network topology adjustments. Parallel lines are modeled efficiently since the real and reactive power flows of each line are considered as problem variables. Limits on reactive power generation, line real power flow and bus voltage magnitudes are presented by (4)–(6), respectively. In the Base Case Network Check, the limit on real power generation (7) is applied to all units except that of slack bus to compensate for power loss mismatch. In the Contingencies Network Check, (8) is applied to consider the unit real power generation adjustments in contingencies. Using the proposed AC power flow equations, the network topology adjustments, i.e., transmission line switching and contingency, can simply be applied by modifying (3). Using the proposed formulation, the power injections due to FACTS devices are added to (2) and unit contingencies are considered by modifying (4) and (8). Further details on the proposed formulation are provided in the following subsection.

2.3. Network check (detailed formulation)

Once the initial unit and line schedule is determined by the UC problem, the Base Case Network Check subproblem is solved for 24 h. In this subproblem, slack variables for real and reactive power mismatches at various buses are considered for minimization to check whether a converged AC power flow solution can be obtained based on UC results.

$$Min\,w_t^c = \sum_{b=1}^{NB}\left(MP_{bt,1}^c + MP_{bt,2}^c\right) + \sum_{b=1}^{NB}\left(MQ_{bt,1}^c + MQ_{bt,2}^c\right) \tag{9}$$

Table 1
Power injection model components of FACTS devices.

Controller type	FACTS device	Steady state function	Control variable
Series	TCPS TCSC SSSC	Real power flow control	PF^{se}
Shunt	SVC STATCOM	Voltage regulation	QF^{sh}
Shunt-series	UPFC	Real and reactive power flow control Voltage regulation	PF^{Se}, QF^{Se}, QF^{sh}

The constraints are given as follows:

$$z_{lt}^{c} = \hat{z}_{lt}^{c} \leftrightarrow \mu_{lt}^{c} \quad (l = 1, \ldots, NS) \tag{10}$$

$$\sum_{i \in U_b} \Delta P_{it}^{c} - \sum_{l \in L_b^s} \Delta PL_{lt}^{sc} - \sum_{l \in L_b^{ns}} \Delta PL_{lt}^{nsc} + MP_{bt,1}^{c} - MP_{bt,2}^{c} = dP_{0bt}^{c} \quad (b = 1, \ldots, NB) \tag{11}$$

$$\sum_{i \in U_b} \Delta Q_{it}^{c} - \sum_{l \in L_b^s} \Delta QL_{lt}^{sc} - \sum_{l \in L_b^{ns}} \Delta QL_{lt}^{nsc} + MQ_{bt,1}^{c} - MQ_{bt,2}^{c} = dQ_{0bt}^{c} \quad (b = 1, \ldots, NB) \tag{12}$$

$$\Delta Q_{it}^{c\min} \widehat{I}_{it} \leqslant \Delta Q_{it}^{c} \leqslant \Delta Q_{it}^{c\max} \widehat{I}_{it} \leftrightarrow \underline{\psi}_{it}^{c}, \bar{\psi}_{it}^{c} \quad (i = 1, \ldots, NG) \tag{13}$$

$$\Delta V_{bt}^{c\min} \leqslant \Delta V_{bt}^{c} \leqslant \Delta V_{bt}^{c\max} \quad (b = 1, \ldots, NB) \tag{14}$$

$$\Delta PL_{lt}^{nsc} - \sum_{b=1}^{NB} \frac{\partial PL_{lt}^{nsc}}{\partial \theta_{bt}^{c}} \Delta \theta_{bt}^{c} - \sum_{b=1}^{NB} \frac{\partial PL_{lt}^{nsc}}{\partial V_{bt}^{c}} \Delta V_{bt}^{c} \leqslant M(1 - UY_{lt}^{c}) \quad (l = 1, \ldots, NNS) \tag{15}$$

$$\Delta PL_{lt}^{nsc} - \sum_{b=1}^{NB} \frac{\partial PL_{lt}^{nsc}}{\partial \theta_{bt}^{c}} \Delta \theta_{bt}^{c} - \sum_{b=1}^{NB} \frac{\partial PL_{lt}^{nsc}}{\partial V_{bt}^{c}} \Delta V_{bt}^{c} \geqslant -M(1 - UY_{lt}^{c}) \quad (l = 1, \ldots, NNS) \tag{16}$$

$$-\Delta PL_{lt}^{c\max} UY_{lt}^{c} \leqslant \Delta PL_{lt}^{nsc} \leqslant \Delta PL_{lt}^{c\max} UY_{lt}^{c} \quad (l = 1, \ldots, NNS) \tag{17}$$

$$\Delta QL_{lt}^{nsc} - \sum_{b=1}^{NB} \frac{\partial QL_{lt}^{nsc}}{\partial \theta_{bt}^{c}} \Delta \theta_{bt}^{c} - \sum_{b=1}^{NB} \frac{\partial QL_{lt}^{nsc}}{\partial V_{bt}^{c}} \Delta V_{bt}^{c} \leqslant M(1 - UY_{lt}^{c}) \quad (l = 1, \ldots, NNS) \tag{18}$$

$$\Delta QL_{lt}^{nsc} - \sum_{b=1}^{NB} \frac{\partial QL_{lt}^{nsc}}{\partial \theta_{bt}^{c}} \Delta \theta_{bt}^{c} - \sum_{b=1}^{NB} \frac{\partial QL_{lt}^{nsc}}{\partial V_{bt}^{c}} \Delta V_{bt}^{c} \geqslant -M(1 - UY_{lt}^{c}) \quad (l = 1, \ldots, NNS) \tag{19}$$

$$\Delta PL_{lt}^{sc} - \sum_{b=1}^{NB} \frac{\partial PL_{lt}^{sc}}{\partial \theta_{bt}^{c}} \Delta \theta_{bt}^{c} - \sum_{b=1}^{NB} \frac{\partial PL_{lt}^{sc}}{\partial V_{bt}^{c}} \Delta V_{bt}^{c} \leqslant M(2 - z_{lt}^{c} - UY_{lt}^{c}) \quad (l = 1, \ldots, NS) \tag{20}$$

$$\Delta PL_{lt}^{sc} - \sum_{b=1}^{NB} \frac{\partial PL_{lt}^{sc}}{\partial \theta_{bt}^{c}} \Delta \theta_{bt}^{c} - \sum_{b=1}^{NB} \frac{\partial PL_{lt}^{sc}}{\partial V_{bt}^{c}} \Delta V_{bt}^{c} \geqslant -M(2 - z_{lt}^{c} - UY_{lt}^{c}) \quad (l = 1, \ldots, NS) \tag{21}$$

$$-\Delta PL_{lt}^{c\max} z_{lt}^{c} UY_{lt}^{c} \leqslant \Delta PL_{lt}^{sc} \leqslant \Delta PL_{lt}^{c\max} z_{lt}^{c} UY_{lt}^{c} \quad (l = 1, \ldots, NS) \tag{22}$$

$$\Delta QL_{lt}^{sc} - \sum_{b=1}^{NB} \frac{\partial QL_{lt}^{sc}}{\partial \theta_{bt}^{c}} \Delta \theta_{bt}^{c} - \sum_{b=1}^{NB} \frac{\partial QL_{lt}^{sc}}{\partial V_{bt}^{c}} \Delta V_{bt}^{c} \leqslant M(2 - z_{lt}^{c} - UY_{lt}^{c}) \quad (l = 1, \ldots, NS) \tag{23}$$

$$\Delta QL_{lt}^{sc} - \sum_{b=1}^{NB} \frac{\partial QL_{lt}^{sc}}{\partial \theta_{bt}^{c}} \Delta \theta_{bt}^{c} - \sum_{b=1}^{NB} \frac{\partial QL_{lt}^{sc}}{\partial V_{bt}^{c}} \Delta V_{bt}^{c} \geqslant -M(2 - z_{lt}^{c} - UY_{lt}^{c}) \quad (l = 1, \ldots, NS) \tag{24}$$

$$-Mz_{lt}^{c} UY_{lt}^{c} \leqslant \Delta QL_{lt}^{sc} \leqslant Mz_{lt}^{c} UY_{lt}^{c} \quad (l = 1, \ldots, NS) \tag{25}$$

$$\Delta \delta_{lt}^{c\min} \leqslant \Delta \theta_{mt}^{c} - \Delta \theta_{nt}^{c} \leqslant \Delta \delta_{lt}^{c\max} \tag{26}$$

In (10), $\hat{z}_{lt}^{c}$ is the fixed value calculated by UC for Benders cuts. In power mismatch Eqs. (11) and (12), slack variables would model system violations. Slack variables can be considered as virtual generators/loads that are added to each bus to mitigate mismatches. The right hand-side of (11) and (12) are the present value of power mismatch. Limits on reactive power generations and bus voltage magnitudes are presented by (13) and (14), respectively. The change in real and reactive power flows of non-switchable lines are obtained by (15)–(19). Considering the state of each switchable line, the change in switchable line flows are obtained by (20)–(25). These changes are used to update flows of switchable and non-switchable lines. The standing phase angle difference constraint is considered by (26). Note that $c = 0$ denotes the base case. In (10) and (13), the double arrow refers to the duality of the equality constraint, where μ_{lt}^{c} and ψ_{it}^{c} represent the dual variable (simplex multiplier) of these constraints. Mathematically, a dual variable represents the marginal increment/decrement of the objective value when the variable is changed. When the state of the switchable line is zero the real power flow equation of that line will be relaxed by (20) and (21). Similarly, the reactive power flow equation will be relaxed by (23) and (24). In addition, the change in real and reactive power flows of that line will be set to zero by (22) and (25), respectively. So, the switched line will be completely removed from the system. M is a large positive constant and is calculated as proposed in [12].

For the base case, (27) is added to consider limits on real power generation. This constraint applies to all units except that of the slack bus, which is relaxed to compensate power loss calculations.

$$\Delta P_{it}^{0} = 0 \leftrightarrow \pi_{it}^{0} \quad (i = 2, \ldots, NG) \tag{27}$$

In the case of contingencies, the adjustment range for unit generation at contingency with respect to the base case generation is considered. This constraint is presented by (28).

$$\Delta \Lambda_{it}^{\min} \leqslant \Delta P_{it}^{c} \leqslant \Delta \Lambda_{it}^{\max} \leftrightarrow \underline{\pi}_{it}^{c}, \bar{\pi}_{it}^{c} (i = 2, \ldots, NG) \tag{28}$$

In (28), only contingencies are considered, i.e., $c \geqslant 1$. For the limits on allowable post-contingency power generation redispatch we would have

$$\Delta \Lambda_{it}^{\max} = \Lambda_{i} - \left(P_{it}^{c} - P_{it}^{0}\right) \tag{29}$$

$$\Delta \Lambda_{it}^{\min} = -\Lambda_{i} - \left(P_{it}^{c} - P_{it}^{0}\right) \tag{30}$$

These limits define the maximum allowable adjustments of power generation output in case of contingencies. In the proposed formulation, small changes in state and control variables are subject to variable limits (31)–(36).

$$\Delta Q_{it}^{c\,\min} = Q_i^{\min} - Q_{it}^c \tag{31}$$

$$\Delta Q_{it}^{c\,\max} = Q_i^{\max} - Q_{it}^c \tag{32}$$

$$\Delta V_{bt}^{c\,\min} = V_b^{\min} - V_{bt}^c \tag{33}$$

$$\Delta V_{bt}^{c\,\max} = V_b^{\max} - V_{bt}^c \tag{34}$$

$$\Delta PL_{lt}^{c\,\min} = -PL_l^{\max} - PL_{lt}^c \tag{35}$$

$$\Delta PL_{lt}^{c\,\max} = PL_l^{\max} - PL_{lt}^c \tag{36}$$

The limits on standing phase angle difference are given as (37)–(40).

$$\Delta\delta_{lt}^{0\,\min} = -\delta_l^{\max} - \left(\theta_{mt}^0 - \theta_{nt}^0\right) - Mz_{l(t-1)}^0 - M\left(1 - z_{lt}^0\right) \tag{37}$$

$$\Delta\delta_{lt}^{0\,\max} = \delta_l^{\max} - \left(\theta_{mt}^0 - \theta_{nt}^0\right) + Mz_{l(t-1)}^0 + M\left(1 - z_{lt}^0\right) \tag{38}$$

$$\Delta\delta_{lt}^{c\,\max} = Min\left\{\begin{array}{l}\delta_l^{\max} - \left(\theta_{mt}^c - \theta_{nt}^c\right) + Mz_{l(t-1)}^c + M\left(1 - z_{lt}^c\right),\\ \delta_l^{\max} - \left(\theta_{mt}^c - \theta_{nt}^c\right) + Mz_{lt}^0 + M\left(1 - z_{lt}^c\right)\end{array}\right\} \tag{39}$$

$$\Delta\delta_{lt}^{c\,\min} = -Max\left\{\begin{array}{l}\delta_l^{\max} + \left(\theta_{mt}^c - \theta_{nt}^c\right) + Mz_{l(t-1)}^c + M(1 - z_{lt}^c),\\ \delta_l^{\max} + \left(\theta_{mt}^c - \theta_{nt}^c\right) + Mz_{lt}^0 + M\left(1 - z_{lt}^c\right)\end{array}\right\} \tag{40}$$

In (39) and (40), where $c \geqslant 1$, the minimum and the maximum allowable changes in the standing phase angle difference would depend on the state of a switchable line in successive hours. In the case of contingencies, minimum and maximum allowable changes in the standing phase angle difference are determined based on two different modes of operation. The first mode represents the switchable line state at successive hours in that contingency, where excessive standing phase angle difference may exist when closing the line. The second mode represents the transition from the base case to a contingency. When a line is off at the base case and is switched back on in a contingency case, the standing phase angle difference of the line is checked. We calculate the proper limits on changes of standing phase angle difference by comparing the values in these two modes.

To consider FACTS devices, (11) and (12) are modified since the proposed injections only appear in power mismatch equations at each bus. So, (11) is replaced by (41) and (12) is replaced by (42).

$$\sum_{i\in I_b}\Delta P_{it}^c - \sum_{l\in L_b^s}\Delta PL_{lt}^{sc} - \sum_{l\in L_b^{ns}}\Delta PL_{lt}^{nsc} + \sum_{b\in B_b}\alpha_{b,1}\Delta PF_{bt}^{Se,c} + MP_{bt,1}^c - MP_{bt,2}^c = dP_{0bt}^c \quad (b = 1,\ldots,NB) \tag{41}$$

$$\sum_{i\in I_b}\Delta Q_{it}^c - \sum_{l\in L_b^s}\Delta QL_{lt}^{sc} - \sum_{l\in L_b^{ns}}\Delta QL_{lt}^{nsc} + \sum_{b\in B_b}\alpha_{b,2}\Delta QF_{bt}^{Se,c} + \sum_{b\in B_b}\alpha_{b,3}\Delta QF_{bt}^{Sh,c} + MQ_{bt,1}^c - MQ_{bt,2}^c = dQ_{0bt}^c \quad (b = 1,\ldots,NB) \tag{42}$$

In the above formulations, coefficients are set to represent certain types of FACTS devices as follows [28,29]:

Shunt controller: $\alpha_1 = 0, \alpha_2 = 0, \alpha_3 = 1$.

Series controller: $\alpha_1 = 1, \alpha_2 = 0, \alpha_3 = 0$.

Shunt-series controller: $\alpha_1 = 1, \alpha_2 = 1, \alpha_3 = 1$.

In every iteration, the FACTS control parameter limits are converted into associated PIM values for satisfying the operating constraints.

In the Base Case Network Check, if the total mismatch is greater than zero, the Benders cut (43) is formed and added to the master problem for the next iteration. The violation indicates that the existing UC solution cannot provide a feasible AC power flow solution. The required dual values that would generate cuts are obtained from (27) for power generation, from (13) for commitment state, and from (10) for switchable lines states.

$$\hat{w}_t^0 + \sum_{i=1}^{NG}\pi_{it}^0\left(P_{it}^0 I_{it} - \widehat{P}_{it}^0\widehat{I}_{it}\right) + \sum_{i=1}^{NG}\left(\bar{\psi}_{it}^0 Q_i^{\max} - \underline{\psi}_{it}^0 Q_i^{\min}\right)(I_{it} - \widehat{I}_{it}) + \sum_{l=1}^{NL}\mu_{lt}^0\left(z_{lt}^0 - \hat{z}_{lt}^0\right) \leqslant 0 \tag{43}$$

where $\hat{w}_t^0$ is the current value of (9) in the base case. The number of Benders cuts is equal to the number of hours with power flow violations. These cuts provide proper signals for the convergence of AC power flow by recalculating the hourly UC, dispatch, and the state of switchable lines in the next UC iteration. This iterative process stops when the base case violations are mitigated. In this case, the problem proceeds to the next step to consider different contingencies. In the Contingencies Network Check, if the total mismatch is greater than zero, the Benders cut (44) will be formed for the associated contingency in that hour and added to the UC for the next iteration.

$$\hat{w}_t^c + \sum_{i=1}^{NG}\left(\bar{\pi}_{it}^c - \underline{\pi}_{it}^c\right)\left(P_{it}^0 - \widehat{P}_{it}^0\right) + \sum_{i=1}^{NG}\left(\bar{\psi}_{it}^c Q_i^{\max} - \underline{\psi}_{it}^c Q_i^{\min}\right)(I_{it} - \widehat{I}_{it}) + \sum_{l=1}^{NL}\mu_{lt}^c\left(z_{lt}^c - \hat{z}_{lt}^c\right) \leqslant 0 \tag{44}$$

where $\hat{w}_t^c$ is the current value of (9) in the case of contingencies. The following iterative procedure would provide the solution to the subproblems:

(1) Calculate initial bus mismatches based on the UC solution and initial system states and settings.
(2) Use linear programming (LP) to minimize (9) and calculate changes in system state and control variables (i.e., ΔQ, $\Delta\theta$, ΔV).
(3) Update state and control variables, and calculate bus mismatches.
(4) Again use LP to minimize (9) and calculate changes in the system state and control variables. If the difference between current and previous iterative changes is less than a specified threshold, stop the process. Otherwise, go back to Step 3.

3. Numerical simulations

A modified IEEE 118-bus system, shown in Fig. 3, is analyzed to illustrate the performance of the proposed model. The proposed model was implemented on a 2.4-GHz personal computer using CPLEX 11.0 [30]. This system has 118 buses, 54 units and 186 branches. The data for this system is found in motor.ece.iit.edu/data/SCUC_118test.xls. Twenty lines are considered switchable as shown in Table 2. Outages of unit 28, line 127, and line 136 are considered as credible contingencies. Standing phase angle difference limit of 20° is considered for switchable lines. Three cases are considered as follows:

Case 1: Base case UC without network constraints.
Case 2: Consider real network constraints in the SCUC solution with TS (DC solution).
Case 3: Consider real and reactive network constraints in the SCUC solution with TS (AC solution).

Case 1: In this case, UC will determine the base case schedule of units, when disregarding the network constraints. Seventeen units

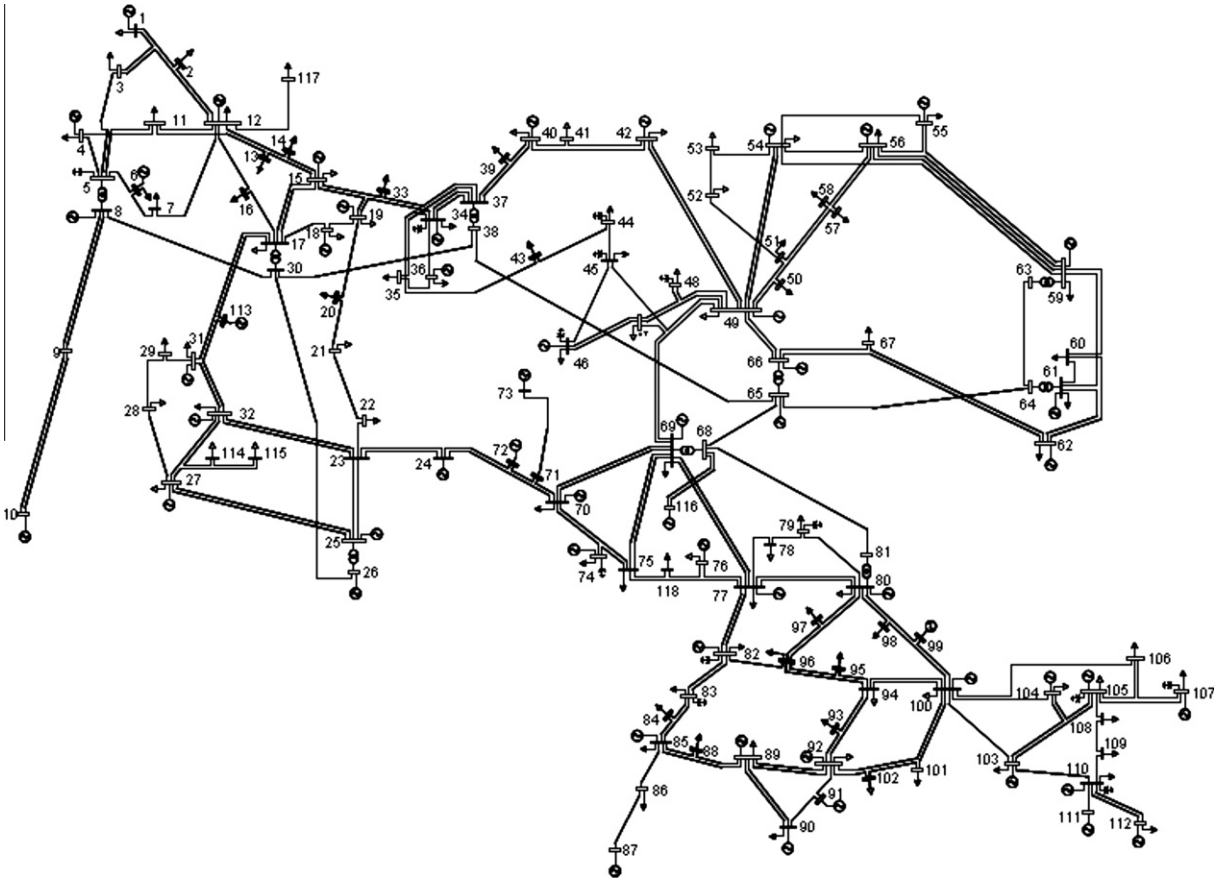

Fig. 3. IEEE 118-bus system.

Table 2
Switchable line data.

Line no.	From bus	To bus	*R* (pu)	*X* (pu)	Charging (pu)	Flow limit (MW)
3	4	5	0.002	0.008	0.002	500
12	11	12	0.006	0.020	0.005	100
16	11	13	0.022	0.073	0.019	100
23	17	18	0.012	0.051	0.013	100
30	23	24	0.014	0.049	0.050	100
40	29	31	0.011	0.033	0.008	100
43	27	32	0.023	0.076	0.019	100
59	43	44	0.061	0.245	0.061	100
67	42	49	0.072	0.323	0.086	100
75	49	54	0.073	0.289	0.074	100
78	54	56	0.003	0.010	0.007	100
90	60	61	0.003	0.014	0.015	500
100	62	66	0.048	0.218	0.058	100
115	70	75	0.043	0.141	0.036	100
151	80	97	0.018	0.093	0.025	100
153	80	99	0.045	0.206	0.055	100
159	99	100	0.018	0.081	0.022	100
164	100	104	0.045	0.204	0.054	100
167	100	106	0.061	0.229	0.062	100
181	27	115	0.016	0.074	0.020	100

are committed at various hours to satisfy the forecasted load. Thirteen economical units are considered as base units, which are committed at the entire scheduling horizon. The other more expensive units are committed whenever necessary to meet the changes in the system load. The UC solution is obtained in 20s with a total operating cost of $792,509.

Case 2: In this case, the hourly SCUC solution is considered with the DC model of the network. The unit schedule is shown in Table 3. In DC network model, voltage magnitudes at system buses are set to 1 and lines resistances are assumed to be zero. Consequently, the reactive load, reactive power generation capability of units and reactive power flow in the system are disregarded. The hourly schedule is quite different from that of Case 1, where the schedule for eleven units is changed. Most changes have occurred at the peak hour, i.e., hour 16, and its adjacent hours. At these hours, units 14, 19, 30, 34, 35 and 37 are turned on and unit 40 is turned

off. Here, the generating unit 40 is turned off for economic reasons. The switchable line states are changed during scheduling hours to mitigate the system congestion and consequently increase the dispatch of economical units. The base case schedule for switchable lines is shown in Table 4, where seventeen switchable lines have changed their hourly states. Lines 90, 115 and 153 are in service at every hour, so their switching capability is not used in the problem solution. At the peak hour, only lines 75 and 164 are switched off to decrease the flow on lines 7, 9, 129, when all other lines are utilized to supply loads. The system contingencies are handled with corrective actions (generation redispatch and TS). The standing phase angle difference of switched lines is checked whenever a line is switched back on, e.g., hour 7 for line 3, hours 7 and 11 for line 12, and so on. Here, none of the lines would exceed their standing phase angle difference limits, so it would be possible to switch the lines back as scheduled. The total operating cost is $802,170, which shows a 1.22% increase in cost in comparison to that in Case 1. This increase is due to consideration of DC model of the network. This DC solution is obtained in 60 s.

Case 3: In this case, the hourly SCUC solution is considered with the AC model of the network. The AC network model would include real and reactive power constraints. The constraints on bus voltage magnitudes are considered in this case. Table 3 highlights the revised hourly state of twenty units as compared to those in Case 2. In this case, most solution changes have occurred close to peak hours, except for units 43 and 44. Unit 43 is on at every hour to prevent voltage drops at buses 93, 94 and 102, and unit 44 is off for economic reasons. The switchable line schedule is shown in Table 5. Fifteen lines are switched hourly to satisfy the system constraints. The other five lines are switched at some hours. TS would increase the power transfer capability that could lead to hourly UC changes. TS would also adjust bus voltages and the reactive power dispatch of generating units by changing the network topology. The additional reactive power generated at the peak hour would lead to an overall increase in bus voltage magnitudes. At the peak hour, the smallest voltage magnitude is 0.97 at buses 44, 45, 109 and 118. On the other hand, 17 buses have already reached their upper limits which are adjusted subsequently by TS. TS would also influence voltages at other hours; however these changes do not have a significant effect on the system voltage profile as voltage magnitudes remain within their permissible limits. Fig. 4 depicts the voltage profile at bus 88 with and without TS. The bus is connected to generating units 38 and 40 at buses 85 and 89. Therefore, the two generating units would have the highest impact on the adjustment of voltage at bus 88. However, unit 38 is off and will not have an impact on the voltage at bus 88. We consider two alternatives as follows.

- *Without TS*: Unit 40 is committed at hours 9–18. In this case, the voltage magnitude at bus 88 is at its lower limit at hours 3–6 and close to its upper limit at hours 10 and 13–18. At hour 9, the voltage magnitude at bus 88 increases when unit 40 is committed. At hour 11, the voltage at bus 88 is affected by the

Table 3
UC schedule of IEEE 118-bus system in case 2.

Unit	Hours (1–24)																							
1–3	0	0	0	0	0	0	0	0	0	0	0	0	0	0	0	0	0	0	0	0	0	0	0	0
4	0	0	0	0	0	0	0	0	1	1	1	1	1	1	1	1	1	1	1	1	1	1	1	1
5	1	1	1	1	1	1	1	1	1	1	1	1	1	1	1	1	1	1	1	1	1	1	1	1
6	0	0	0	0	0	0	0	0	0	0	0	0	0	0	0	0	0	0	0	0	0	0	0	0
7	0	0	0	0	0	0	0	0	0	0	0	0	0	0	0	0	0	0	0	0	0	0	0	0
8–9	0	0	0	0	0	0	0	0	0	0	0	0	0	0	0	0	0	0	0	0	0	0	0	0
10–11	1	1	1	1	1	1	1	1	1	1	1	1	1	1	1	1	1	1	1	1	1	1	1	1
12–13	0	0	0	0	0	0	0	0	0	0	0	0	0	0	0	0	0	0	0	0	0	0	0	0
14	0	0	0	0	0	0	0	0	0	0	0	0	1	1	1	1	1	0	0	0	0	0	0	0
15	0	0	0	0	0	0	0	0	0	0	0	0	0	0	0	0	0	0	0	0	0	0	0	0
16	0	0	0	0	0	0	0	0	0	0	0	0	0	0	0	0	0	0	0	0	0	0	0	0
17–18	0	0	0	0	0	0	0	0	0	0	0	0	0	0	0	0	0	0	0	0	0	0	0	0
19	0	0	0	0	0	0	0	0	0	0	0	0	0	0	1	1	1	1	1	1	0	0	0	0
20–21	1	1	1	1	1	1	1	1	1	1	1	1	1	1	1	1	1	1	1	1	1	1	1	1
22	0	0	0	0	0	0	0	0	0	0	0	0	0	0	0	0	0	0	0	0	0	0	0	0
23	0	0	0	0	0	0	0	0	0	0	0	0	0	0	0	0	0	0	0	0	0	0	0	0
24–25	1	1	1	1	1	1	1	1	1	1	1	1	1	1	1	1	1	1	1	1	1	1	1	1
26	0	0	0	0	0	0	0	0	0	0	0	0	0	0	0	0	0	0	0	0	0	0	0	0
27–29	1	1	1	1	1	1	1	1	1	1	1	1	1	1	1	1	1	1	1	1	1	1	1	1
30	0	0	0	0	0	0	0	0	0	0	1	1	1	1	1	1	1	1	1	1	1	1	0	0
31	0	0	0	0	0	0	0	0	0	0	0	0	0	0	0	0	0	0	0	0	0	0	0	0
32–33	0	0	0	0	0	0	0	0	0	0	0	0	0	0	0	0	0	0	0	0	0	0	0	0
34	0	0	0	0	0	0	0	0	0	0	0	0	0	0	1	1	1	1	1	0	0	0	0	0
35	0	0	0	0	0	0	0	0	0	0	0	0	0	1	1	1	1	1	1	0	0	0	0	0
36	0	0	0	0	0	0	0	0	0	1	1	1	1	1	1	1	1	1	1	1	1	1	1	0
37	0	0	0	0	0	0	0	0	0	0	0	1	1	1	1	1	1	1	1	1	1	1	1	0
38	0	0	0	0	0	0	0	0	0	0	0	0	0	0	0	0	0	0	0	0	0	0	0	0
39	1	1	1	1	1	1	1	1	1	1	1	1	1	1	1	1	1	1	1	1	1	1	1	1
40	0	0	0	0	0	0	0	0	0	0	0	0	0	0	0	0	0	0	0	0	0	0	0	0
41–42	0	0	0	0	0	0	0	0	0	0	0	0	0	0	0	0	0	0	0	0	0	0	0	0
43	0	0	0	0	0	0	0	0	0	0	1	1	1	1	1	1	1	1	1	1	1	1	0	0
44	1	1	1	1	1	1	1	1	1	1	1	1	1	1	1	1	1	1	1	1	1	1	1	1
45	1	1	1	1	1	1	1	1	1	1	1	1	1	1	1	1	1	1	1	1	1	1	1	1
46–47	0	0	0	0	0	0	0	0	0	0	0	0	0	0	0	0	0	0	0	0	0	0	0	0
48	0	0	0	0	0	0	0	0	0	0	0	0	0	0	0	0	0	0	0	0	0	0	0	0
49	0	0	0	0	0	0	0	0	0	0	0	0	0	0	0	0	0	0	0	0	0	0	0	0
50–51	0	0	0	0	0	0	0	0	0	0	0	0	0	0	0	0	0	0	0	0	0	0	0	0
52	0	0	0	0	0	0	0	0	0	0	0	0	0	0	0	0	0	0	0	0	0	0	0	0
53	0	0	0	0	0	0	0	0	0	0	0	0	0	0	0	0	0	0	0	0	0	0	0	0
54	0	0	0	0	0	0	0	0	0	0	0	0	0	0	0	0	0	0	0	0	0	0	0	0

Table 4
Switchable line schedule of IEEE 118-bus system in case 2.

Line	Hours (1–24)																							
3	1	1	1	1	1	0	1	1	1	1	1	1	1	1	1	1	1	1	1	1	1	1	1	1
12	1	1	1	1	1	0	1	1	0	0	1	1	1	1	1	1	1	1	1	1	1	1	1	0
16	1	1	0	0	0	1	1	1	1	1	1	1	1	1	1	1	1	1	1	1	1	1	1	1
23	1	1	1	1	1	0	1	1	1	1	1	1	1	1	1	1	1	1	1	1	1	1	1	1
30	0	0	0	0	0	1	0	0	0	1	0	0	0	0	0	1	0	0	0	0	0	0	1	1
40	0	1	1	1	1	0	0	0	0	1	0	0	0	0	0	1	0	0	0	0	0	0	1	1
43	1	1	1	1	1	0	1	1	1	1	1	1	1	1	1	1	1	1	1	1	1	1	1	1
59	1	1	1	1	1	1	1	1	0	0	0	0	0	0	0	1	0	0	0	0	0	0	0	1
67	1	0	1	1	1	1	1	1	1	1	1	1	1	1	1	1	0	1	1	1	1	1	1	1
75	0	0	1	1	1	1	0	0	0	0	0	0	0	0	0	0	0	0	0	0	0	0	0	0
78	0	0	1	0	0	0	0	0	0	0	0	0	0	0	0	1	0	0	0	0	0	0	0	0
90	1	1	1	1	1	1	1	1	1	1	1	1	1	1	1	1	1	1	1	1	1	1	1	1
100	1	1	1	1	1	1	1	1	1	1	1	0	0	0	0	1	1	0	0	0	0	1	1	1
115	1	1	1	1	1	1	1	1	1	1	1	1	1	1	1	1	1	1	1	1	1	1	1	1
151	0	1	0	1	0	1	0	0	0	0	0	1	1	1	1	1	0	1	1	1	1	0	0	0
153	1	1	1	1	1	1	1	1	1	1	1	1	1	1	1	1	1	1	1	1	1	1	1	1
159	1	0	0	0	0	0	0	1	1	1	0	1	1	1	1	1	1	1	1	1	1	1	0	0
164	1	0	0	0	0	1	0	0	1	0	0	0	0	0	0	0	0	0	1	0	1	0	0	0
167	0	1	1	1	1	1	1	1	1	1	1	1	1	0	1	1	0	1	1	1	1	0	0	1
181	1	1	1	1	1	0	1	1	1	1	1	1	1	1	1	1	1	1	1	1	1	1	1	1

Table 5
Switchable line schedule of IEEE 118-bus system in case 3.

Line	Hours (1–24)																							
3	1	1	1	1	1	1	1	1	0	1	0	1	1	1	1	1	1	1	1	1	1	1	1	0
12	1	1	1	1	1	1	1	1	0	1	0	1	0	0	0	0	0	0	1	0	1	1	1	0
16	1	1	1	1	1	1	0	1	0	1	0	0	0	0	0	0	0	0	0	0	0	0	1	0
23	0	0	0	0	0	0	0	0	0	0	0	0	0	0	0	0	0	0	0	0	0	0	0	0
30	0	0	0	0	0	0	0	0	0	0	0	0	0	0	0	0	0	0	0	0	0	0	0	0
40	0	0	0	0	0	0	0	0	0	0	0	0	0	0	0	0	0	0	0	0	0	0	0	0
43	0	0	0	0	0	0	0	0	0	0	0	0	0	0	0	0	0	0	0	0	0	0	0	0
59	0	0	0	0	0	0	0	0	0	0	0	0	0	0	0	0	0	0	0	0	0	0	0	0
67	0	0	0	0	0	0	0	0	0	0	0	0	0	0	0	0	0	0	0	0	0	0	0	0
75	0	0	0	0	0	0	0	0	0	0	0	0	0	0	0	0	0	0	0	0	0	0	0	0
78	0	0	0	0	0	0	0	0	0	0	0	0	0	0	0	0	0	0	0	0	0	0	0	0
90	0	0	0	0	0	0	0	0	0	0	0	0	0	0	0	0	0	0	0	0	0	0	0	0
100	0	0	0	0	0	0	0	0	0	0	0	0	0	0	0	0	0	0	0	0	0	0	0	0
115	0	0	0	0	0	0	0	0	0	0	0	0	0	0	0	0	0	0	0	0	0	0	0	0
151	0	0	0	0	0	0	0	0	0	0	0	0	0	0	0	0	0	0	0	0	0	0	0	0
153	0	0	0	0	0	0	0	0	0	0	0	0	0	0	0	0	0	0	0	0	0	0	0	0
159	0	0	0	0	0	0	0	0	0	0	0	0	0	0	0	0	0	0	0	0	0	0	0	0
164	1	1	1	1	1	1	1	1	1	1	1	1	1	1	1	1	1	1	1	1	1	1	0	0
167	1	1	1	1	1	1	1	1	1	1	1	1	1	1	1	1	1	1	1	1	1	1	0	0
181	0	0	0	0	0	0	0	0	0	0	0	0	0	0	0	0	0	0	0	0	0	0	0	0

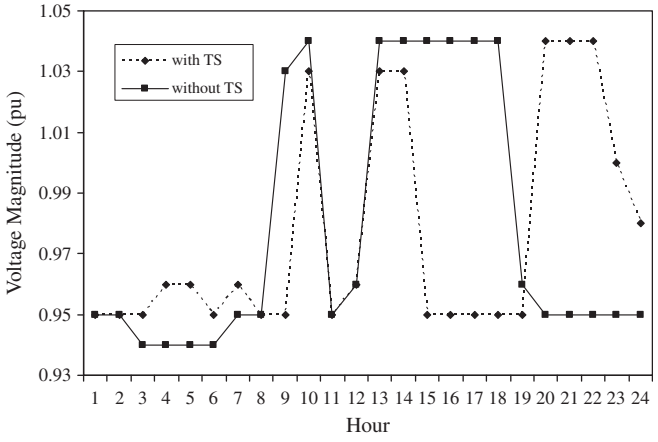

Fig. 4. Voltage profile at bus 88.

change in the UC schedule. At hours 13–18, the voltage magnitude at bus 88 is close to its upper limit. At hours 19–24, the voltage at bus 88 drops because unit 40 which is the local source of voltage adjustment, is not committed.

- *With TS*: Unit 40 is committed at hours 10–22. In this case, the voltage at bus 88 is increased slightly at hours 3–7. The voltage magnitude at bus 88 increases at hour 10 when unit 40 is turned on. The UC adjustments at hour 11 would lead to a voltage magnitude drop at bus 88. At hours 13–14, the reactive power generation of unit 40 would increase the voltage magnitude at bus 88, while the TS application at hours 15–18 would decrease the voltage. The lower real and reactive power generation of unit 40 would decrease the reactive power flow on line 137 and voltage magnitude at bus 88. The commitment of Unit 40 at hours 20–22 would supply the real and reactive power generation which would lead to an increase in the voltage magnitude at bus 88.

TS in Case 3 would provide a better chance for voltage adjustments especially at peak hour. At the peak hours, the additional real and reactive power generation supply the higher load. Using

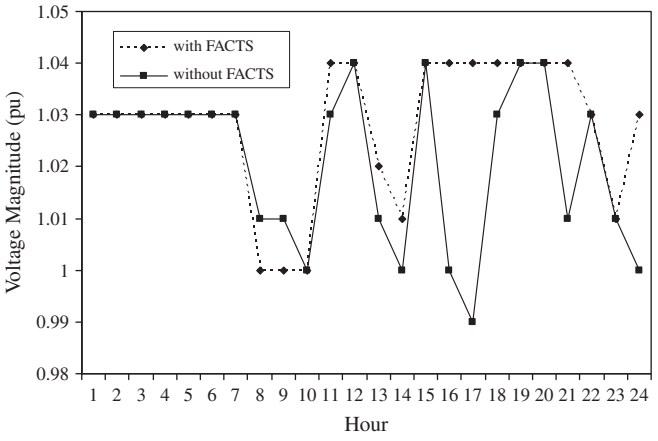

Fig. 5. Voltage profile at bus 68.

TS, voltage magnitudes could be lowered at peak hours which would increase the dispatch of less expensive units for supplying the load.

In Case 3, nine FACTS devices are considered with tap-changing and phase-shifting capabilities. The FACTS devices are modeled using the proposed PIM. In Case 2, where the DC network constraints are considered, the phase-shifting capability of FACTS devices will adjust the real power flow in the associated lines. In Case 3, the FACTS devices would also modify reactive power flows and accordingly adjust bus voltage levels. The FACTS devices generate a counterflow to decrease the power flow on the associated line and therefore increase the transfer capability of the line. The installed FACTS device at line 107 is between buses 68 and 69. The voltage at bus 69 is adjusted by the generating unit located at 29. Without the FACTS device at line 107, the voltage drop might occur at bus 68 mostly at peak hours. However, the reactive power injection to bus 68 increases the bus 68 voltage and prevents voltage violations. Fig. 5 shows the voltage profile of bus 68 with and without FACTS at line 107. Without the FACTS device, voltages are adjusted by the neighboring units 27, 29 and 54. Here, unit 54 is not committed while units 27 and 29 are always committed. The reactive power generation of units 27 and 29 is increased for adjusting the voltage level at bus 68, which would also increase the reactive power flow at connecting lines 104 and 107. The solid line in Fig. 5 shows the adjusted hourly voltage at bus 68. Comparing the two voltage profiles, the voltage deviation is smaller when FACTS devices are in place. So, the FACTS device could reduce the real and reactive power dispatch of units, decrease line flows, and enhance the use of TS. Similar to Case 2, TS would prevent the violation of standing phase angle difference limits. Hence, line flows and bus voltage magnitudes are within their limits when supplying the reactive loads. The total operating cost is $824,342, which is calculated in 162 s.

4. Conclusions

TS was incorporated into the SCUC problem with AC network constraints. To enhance the proposed AC solution of SCUC, FACTS devices were considered. A PIM was used to model the effect of FACTS devices in the AC power flow, using real and reactive power injections to system buses. We concluded that the TS applications would enhance the hourly SCUC solution when considering reactive and voltage constraints. In addition, the incorporation of FACTS devices would further enhance the proposed AC solution of SCUC. The incorporation of AC network constraints would increase the total operating cost and the execution time, which is regarded as a trade-off between more accurate and faster SCUC solutions.

Acknowledgement

This work was supported in part by the United States Department of Energy Grant # DE-EE 0001380.000.

References

[1] Shahidehpour M, Yamin H, Li Z. Market operations in electric power systems. New York: Wiley; 2002.
[2] Conejo AJ, Castillo E, Mínguez R, García-Bertrand R. Decomposition techniques in mathematical programming. Springer; 2006.
[3] Bakirtzis A, Meliopoulos A. Incorporation of switching operation in power system corrective control computations. IEEE Trans Power Syst 1987;7(8):669–76.
[4] Rahimi F, Zhang M, Hobbs B. Competitive transmission path assessment for local market power mitigation. In: Power eng soc gen meeting; 2007.
[5] Granelli G, Montagna M, Zanellini F, Bresesti P, Vailati R, Innorta M. Optimal network reconfiguration for congestion management by deterministic and genetic algorithms. Electr Power Syst Res 2006;76:549–56.
[6] Schnyder G, Glavitsch H. Integrated security control using an optimal power flow and switching concepts. IEEE Trans Power Syst 1988;3(2):782–90.
[7] Schnyder G, Glavitsch H. Security enhancement using an optimal switching power flow. IEEE Trans Power Syst 1990;5(2):674–81.
[8] Rolim JG, Machado LJB. A study of the use of corrective switching in transmission systems. IEEE Trans Power Syst 1999;14(1):336–41.
[9] Wang J, Shahidehpour M, Li Z. Security-constrained unit commitment with volatile wind power generation. IEEE Trans Power Syst 2008;23(3):1319–27.
[10] Khodaei A, Shahidehpour M. Transmission switching in security-constrained unit commitment. IEEE Trans Power Syst 2010;25(4):1937–45.
[11] Tor OB, Guven AN, Shahidehpour M. Congestion-driven transmission planning considering the impact of generator expansion. IEEE Trans Power Syst 2008;23(2):781–9.
[12] Khodaei A, Shahidehpour M, Kamalinia S. Transmission switching in expansion planning. IEEE Trans Power Syst 2010;25(3):1722–33.
[13] Fu Y, Shahidehpour M, Li Z. Security-constrained unit commitment with AC constraints. IEEE Trans Power Syst 2005;20(3):1538–50.
[14] Shahidehpour M, Fu Y. Benders decomposition. IEEE Power Energy Mag 2005;3(2).
[15] Chung KH, Kim BH, Hur D. Multi-area generation scheduling algorithm with regionally distributed optimal power flow using alternating direction method. Int J Electr Power Energy Syst 2011;33(9):1527–35.
[16] Ma H, Shahidehpour M. Transmission constrained unit commitment based on Benders decomposition. Elect Power Energy Syst 1998;20(4):287–94.
[17] Geoffrion AM. Generalized Benders decomposition. J Opt Theory Appl 1972;10(4).
[18] Wood AJ, Wollenberg BF. Power generation, operation and control. New York: Wiley; 1984.
[19] Senthil Kumar V, Mohan MR. Solution to security constrained unit commitment problem using genetic algorithm. Int J Electr Power Energy Syst 2010;32(2):117–25.
[20] Frangioni A, Gentile C, Lacalandra F. Sequential Lagrangian-MILP approaches for Unit Commitment problems. Int J Electr Power Energy Syst 2011;33(3):585–93.
[21] Martins N, Oliviera EJ, Moreira WC, Pereira JLR, Fontoura RM. Redispatch to reduce rotor shaft impacts upon transmission loop closure. IEEE Trans Power Syst 2008;23(2):592–600.
[22] Nagata T, Sasaki H, Yokoyama R. Power system restoration by joint usage of expert system and mathematical programming approach. IEEE Trans Power Syst 1995;10(3):1473–9.
[23] Wunderlich S, Adibi MM, Fischl R, Nwankpa COD. An approach to standing phase angle reduction. IEEE Trans Power Syst 1994;9(1):470–8.
[24] Hazarika D, Sinhá AK. Standing phase angle reduction for power system restoration. Proc Inst Elect Eng, Gen Trans Distr 1998;145(1).
[25] Hazarika D, Sinhá AK. An algorithm for standing phase angle reduction for power system restoration. IEEE Trans Power Syst 1999;14(4):1213–8.
[26] Martins N, Oliveira EJ, Pereira JLR, Ferreira LCA. Reducing standing phase angles via interior point optimum power flow for improved system restoration. In: Proc power syst conf expo 2004, New York; 2004.
[27] Kulworawanichpong T. Simplified Newton–Raphson power-flow solution method. Int J Electr Power Energy Syst 2010;32(6):551–8.
[28] Xiao Y, Song YH, Sun YZ. Versatile model for power flow control using FACTS devices. In: Power elect and motion cont conf; 2000.
[29] Lai LL, Ma JT. Power flow control in FACTS using evolutionary programming. In: IEEE intern conf on evol comp; 1995.
[30] The ILOG CPLEX Website; 2006. <http://www.ilog.com>.